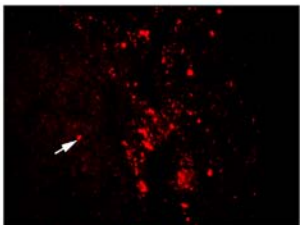
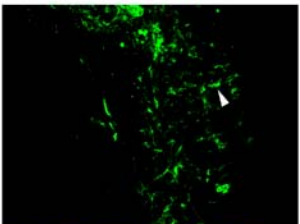


Supplementary Figure 1

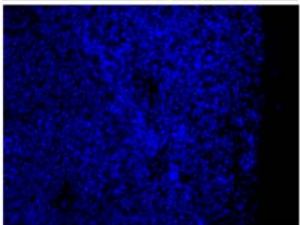
CMTMR
CD34+
cells



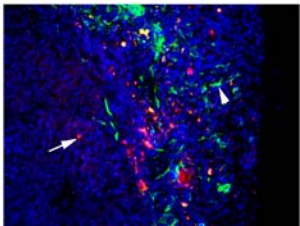
CD31



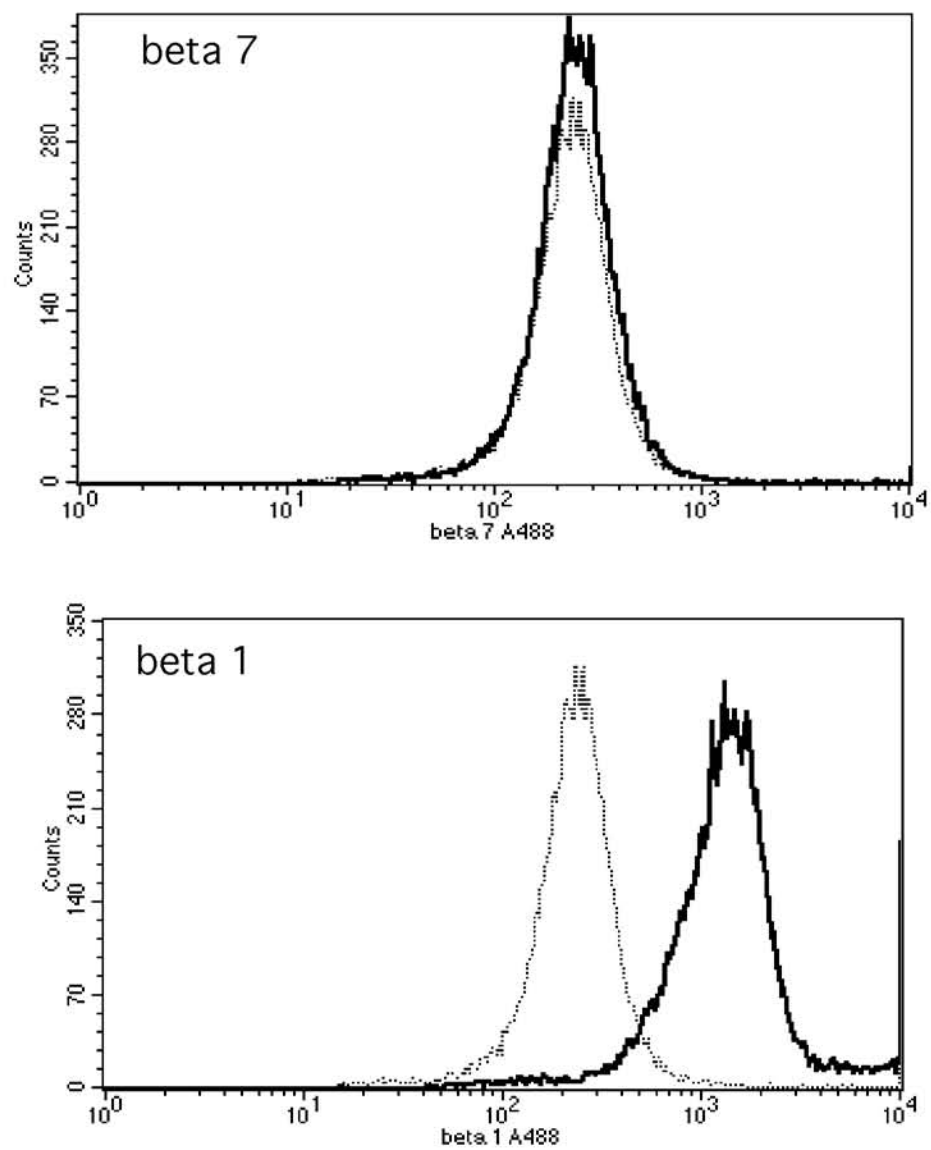
DAPI



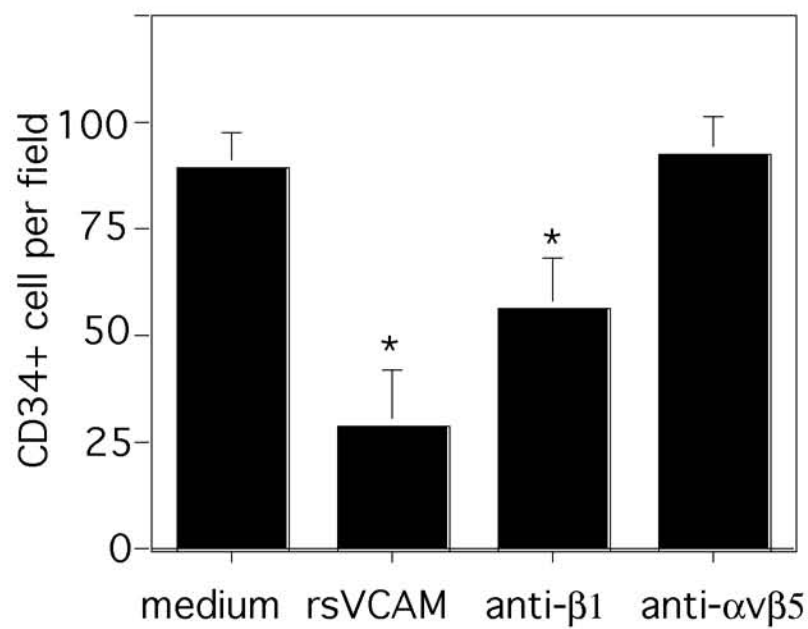
Merge

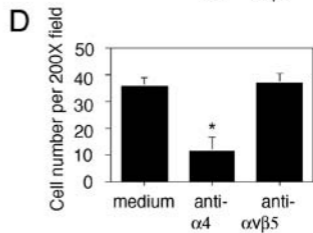
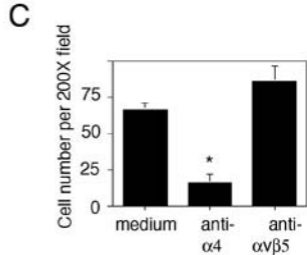
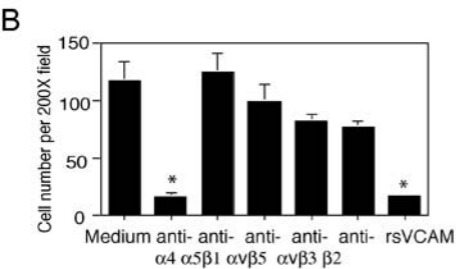
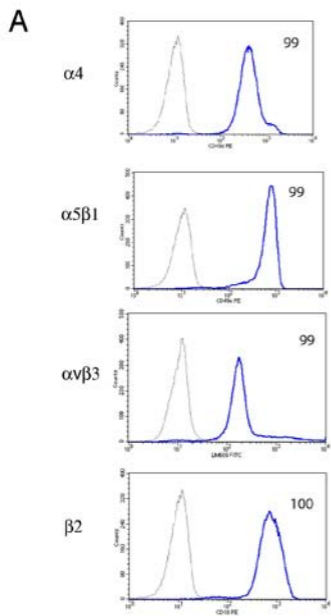


A



B



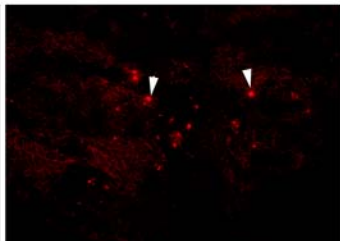
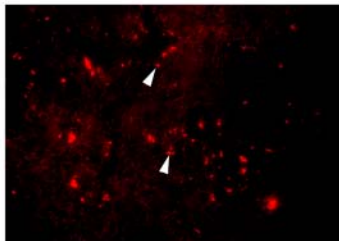


Supplementary Figure 3

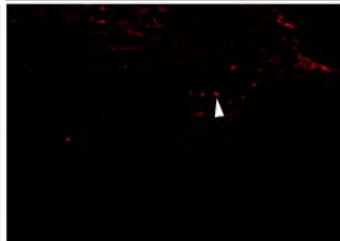
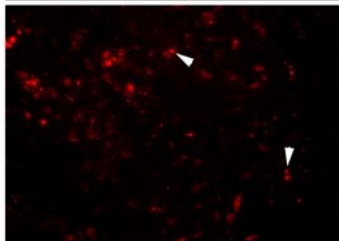
LLC subcutaneous tumor

Lung

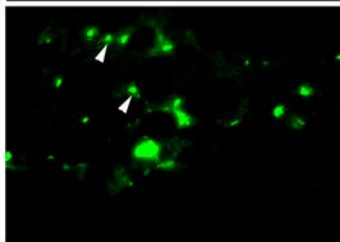
CD34 -



CD34+



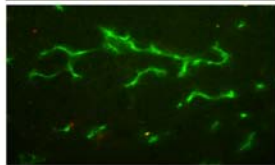
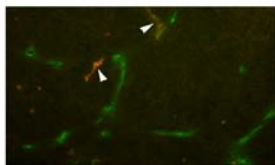
CHO α 4+



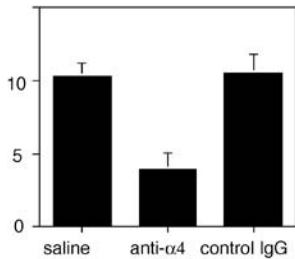
Supplementary Figure 4

A

Control IgG

anti- α 4**B**

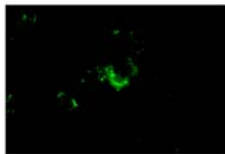
CMTMR positive vessels/field

**C**

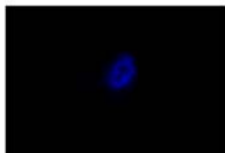
CMTMR



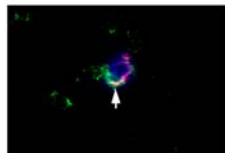
Ki67



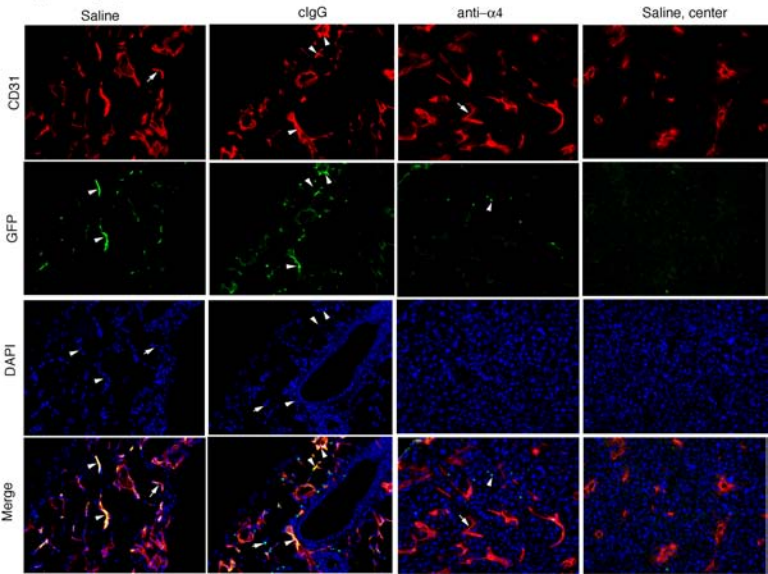
CD31



Merge



Supplementary Figure 6

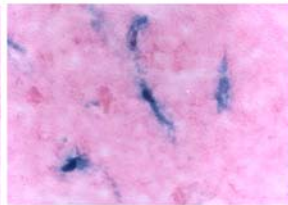
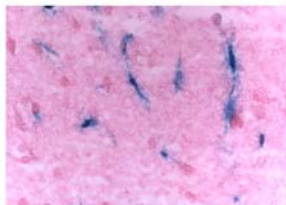
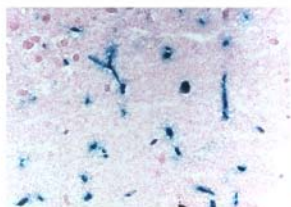


400X

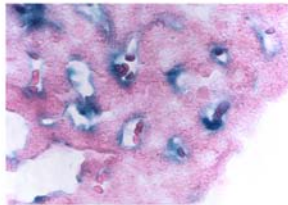
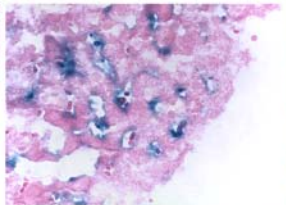
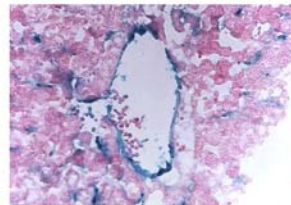
600X

1000X

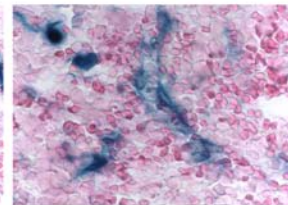
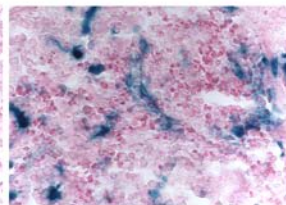
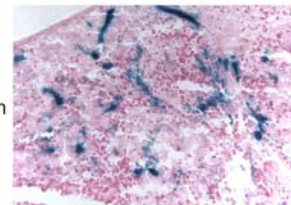
Brain



Liver



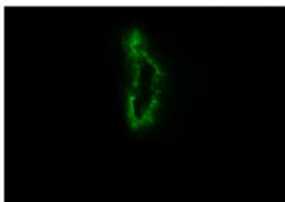
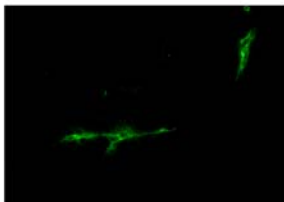
Spleen



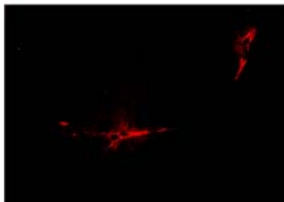
400X

1000X

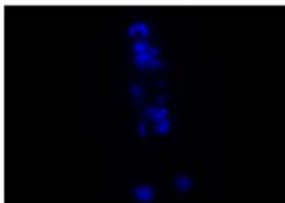
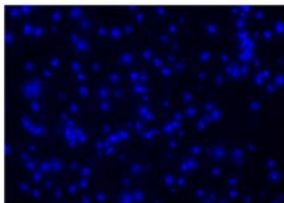
betaGal



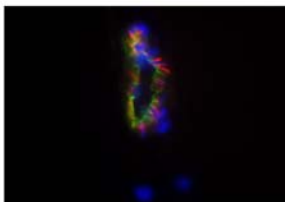
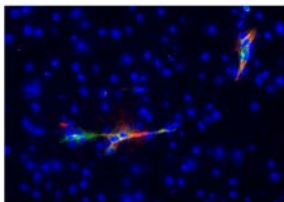
CD31



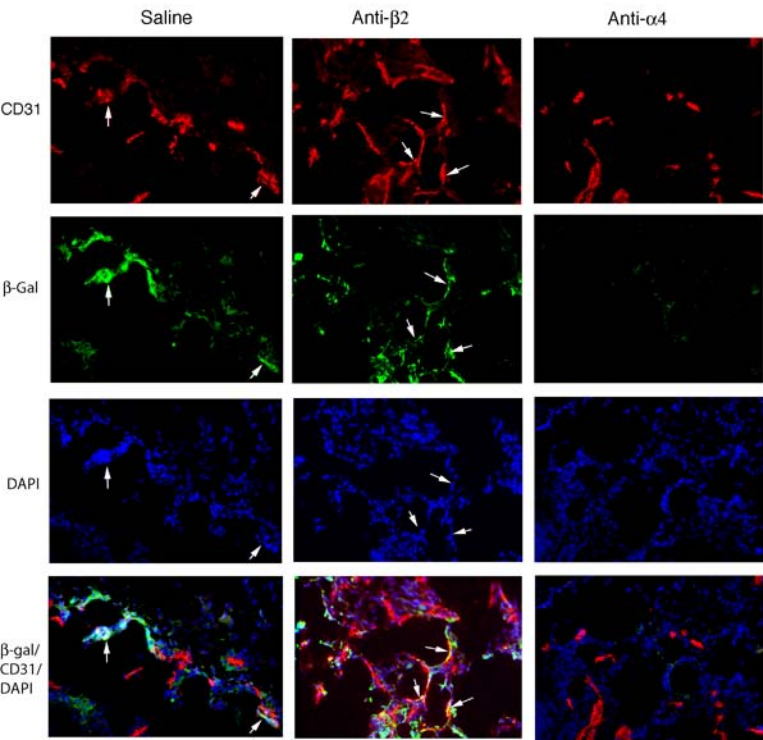
DAPI



Merge



Supplementary Figure 9



Supplementary Figure 1: Individual images of homing of CD34+ cells to tumor periphery. Five micron cryosections of the tumors from animals injected with CD34+ cells (red) were fixed in acetone, then incubated with DAPI (blue), rat anti-mouse CD31 and goat anti-rat FITC antibodies (green) and photographed at magnification 200X. Arrowheads indicate CD34+ cells. Arrows indicate CD31 positive blood vessels. Bar=50 μ m.

Supplementary Figure 2: Expression and function of integrin β 1 and β 7 in human CD34+ cells.

(A) FACS profiles for integrin β 1 and β 7 integrins on circulating CD34- cells. FACS profile in gray represents fluorescence of isotype control antibody. Percent positive cells is indicated by number in right hand corner of each profile.

(B) Average number of CD34- cells adhering to endothelial cell monolayers in the presence of medium, anti- β 1, anti- α v β 5 and rsVCAM per 200X microscopic field +/-SEM. Asterisks indicate $P < 0.01$.

Supplementary Figure 3: Integrin expression and adhesion profiles of human CD34- cells

(A) FACS profiles for integrin α 4 β 1, α 5 β 1, α v β 3 and β 2 integrins on circulating CD34- cells. FACS profile in gray represents fluorescence of isotype control antibody. Percent positive cells is indicated by number in right hand corner of each profile. (B) Average number of CD34- cells adhering to endothelial cell monolayers in the presence of medium, anti- α 4 β 1, anti- α 5 β 1,

anti- α v β 5, anti- α v β 3, anti- β 2 and rsVCAM per 200X microscopic field +/-SEM. Asterisks indicate $P < 0.01$. (C-D) Average number of CD34- cells adhering to CS-1 fibronectin or (D) rsVCAM in the presence of medium, anti- α 4 β 1 or isotype matched control antibody (cIgG, anti- α v β 5) per 200X microscopic field +/-SEM. Asterisks indicate $P < 0.01$.

Supplementary Figure 4: Mouse lung tissue from CD34+ cell injected animals

Subcutaneous Lewis lung carcinoma (LLC) tumors and lung tissue from mice injected with 0.5×10^6 CMTMR labeled CD34- cells, CMTMR labeled CD34+ cells or GFP+ α 4 β 1+ Chinese hamster ovary cells (CHO α 4+). Note that many human CMTMR labeled cells (red, arrowheads) are present in tumors but few are present in lungs. No GFP+ α 4+ CHO cells are present in tumors while many GFP+ cells are present in lungs.

Supplementary Figure 5: CD34+ cell contribution to angiogenesis is integrin α 4 β 1 dependent

(A) Cryosections from mice with subcutaneous HT29 colon carcinoma tumors that were injected with CMTMR labeled CD34+ cells (red) and treated with saline, anti-human integrin α 4 β 1 and anti-human α v β 5 for five days. After five days, animals were injected with fluorescent lectin *Bandeira simplicifolia* to highlight blood vessels (green). (B) Average number +/- SEM of CMTMR positive CD31+ blood vessels per 200x microscopic field for each treatment

group. (C) Cryosections from mice with subcutaneous Lewis lung carcinoma tumors that were injected with CMTMR labeled CD34+ cells (red) and sacrificed seven days later. Expression of Ki67 (green) in CMTMR (red) cells that formed CD31+ blood vessels (blue) in vivo.

Supplementary Figure 6: Lin- cell contribution to angiogenesis

Red (anti-CD31, arrows), green (EGFP, arrowheads) and blue (DAPI) color panels and merged images of cryosections of the periphery or center of LLC tumors from mice injected with EGFP+Lin- cells at 200X magnification. Peripheral tumor sections from animals were treated with saline, isotype matched, control anti-integrin antibodies (cIgG) or anti- $\alpha 4\beta 1$ antibodies are shown in the left three columns, while central tumor sections from saline treated mice are shown in the right column. EGFP+ blood vessels are yellow.

Supplementary Figure 7: Tie2LacZ positive blood vessels

Cryosections from Tie2LacZ mouse brain, liver, and spleen were stained to detect beta-galactosidase (blue) and counterstained with nuclear fast red. Images were captured at 400X, 600X and 1000X magnification.

Supplementary Figure 8: LacZ+ cell contribution to angiogenesis

Green (beta-galactosidase), red (CD31), blue (DAPI) and merged images of cryosections of bFGF saturated Matrigel from mice transplanted with Tie2LacZ bone marrow and treated with saline, anti- $\alpha 4\beta 1$ or control isotype

matched anti-integrin β 2 antibodies (cIgG). Cryosections were immunostained for beta-galactosidase to detect LacZ expressing cells (green), anti-CD31 to detect blood vessels (red) and DAPI to detect nuclei (blue). LacZ+/CD31+ vessels are yellow (arrows).

Supplementary Figure 9: Immunostaining for LacZ+ cell contribution to angiogenesis

Green (beta-galactosidase), red (CD31), blue (DAPI) and merged images of cryosections of Tie2LacZ mouse brain at 400 and 1000X. Cryosections were immunostained for beta-galactosidase to detect LacZ expressing cells (green), anti-CD31 to detect blood vessels (red) and DAPI to detect nuclei (blue). LacZ+/CD31+ vessels are yellow.